

Anisotropic polarizability of isolated semiconducting single-wall carbon nanotubes in alternating electric fields

J. A. Fagan,^{a)} V. Bajpai, B. J. Bauer, and E. K. Hobbie

Polymers Division, National Institute of Standards and Technology, Gaithersburg, Maryland 20899, USA

(Received 21 June 2007; accepted 19 October 2007; published online 21 November 2007)

We measure the linear dichroism for aqueous suspensions of isolated semiconducting single-wall carbon nanotubes (SWCNTs) in alternating electric fields. The field-induced alignment of length-purified SWCNTs is determined from the anisotropy of the first and second interband optical transitions for the (6,5) semiconducting species. At 3 kHz, the effective anisotropic polarizability of the DNA-wrapped SWCNTs is of order 10^{-28} F m², comparable to that of a high-aspect-ratio conducting rod, but a factor of 5 larger than that of gold colloidal rods and an order of magnitude larger than that of tobacco mosaic virus. © 2007 American Institute of Physics.

[DOI: 10.1063/1.2807850]

The remarkable physical properties of single-wall carbon nanotubes (SWCNTs) make them candidates for a host of advanced technologies. In particular, their highly anisotropic optical and electronic characteristics have generated interest in the area of nanoscale transistors, electrochemical electrodes, and flexible conductive films. Individual SWCNTs can be either semiconducting or metallic, the band structure being specified by the chirality index (n, m) that identifies the wrapping vector of the rolled graphene sheet comprising the nanotube.¹ In many potential applications, the ability to isolate and select for both the unique electronic characteristics of a specific chirality and the geometric constraints of a single length will be critical. An important length-dependent electronic characteristic that influences both the dielectrophoretic mobility and the electric-field based alignment of a SWCNT is the anisotropic polarizability. Measurements of this anisotropy are critical to developing schemes that separate and manipulate SWCNTs with electric fields.

Three previous measurements of the anisotropic SWCNT polarizability exist in the literature.²⁻⁴ In each case, the birefringence or dichroism of a nanotube suspension in an external electric field was recorded at a single optical wavelength, which samples the combined response of multiple SWCNT chiralities. Recent advances, such as single-stranded DNA for SWCNT dispersion and size-exclusion chromatography for length sorting, allow for significant improvement. Here, spectroscopic linear dichroism is used to measure the alignment of length-sorted SWCNTs of a specific chirality in response to an oscillating electric field, and the anisotropic polarizability of the DNA-wrapped (6,5) semiconducting SWCNT extracted.

The application of a spatially uniform electric field to a solution of dispersed particles with anisotropic polarizability induces an orienting force on the particles. At the frequency of interest here, the polarization is expected to be in phase with the applied field. For rigid rods without a permanent dipole, the interaction energy is⁵

$$U(\theta) = -\frac{1}{2}(\alpha_{\parallel} - \alpha_{\perp})E^2 \cos^2 \theta, \quad (1)$$

where α_{\parallel} and α_{\perp} are the axial and transverse excess polarizabilities of the SWCNT ($\Delta\alpha = \alpha_{\parallel} - \alpha_{\perp}$), E is the electric field,

and θ is the angle between the long axis of the SWCNT and the direction of E . Invoking Boltzmann's equation, O'Konski *et al.*⁶ solved for the steady-state uniaxial distribution of rods in response to a static field,

$$f(\theta) = \frac{e^{-U(\theta)/k_B T}}{\int_0^{\pi} e^{-U(\theta)/k_B T} \sin \theta d\theta}, \quad (2)$$

where k_B is Boltzmann's constant and T is the temperature. The extent of alignment is quantified by $S = \langle P_2(\cos \theta) \rangle$, where $P_2(x) = (3x^2 - 1)/2$ is the second Legendre polynomial and $\langle \cdot \cdot \rangle$ denotes an average over $f(\theta)$. The order parameter S is 0 for a random distribution of orientations and 1 for perfect alignment along $\theta = 0$. To extend Eqs. (1) and (2) to a time varying field, E is replaced by its time average, E_{rms} .

The dichroism for a given alignment is related to the orientational anisotropy of the absorption feature being observed.⁷ Since the optical anisotropy of the absorption peaks and any background contribution are potentially different, a determination of S based solely on the dichroism must treat each part independently. For two orientation-susceptible contributions with a nonsusceptible background, the total absorbance will be

$$A(\theta, \lambda) = A_1(\theta, \lambda) + A_2(\theta, \lambda) + A_3(\lambda), \quad (3)$$

in which A_1 is the peak absorption, A_2 is the broad background (π -plasmon) absorption,⁷ and A_3 is a nonsusceptible background. For the length fractionated SWCNTs used here, A_2 is small compared to A_1 in the wavelength range of the first interband transition (denoted 11), and of approximately equal weight in the range of the second interband transition (denoted 22). A_3 is negligible for the sample of interest. For a rigid rod with large absorption anisotropy, the absorption is related to S by $S_{i=1,2} \approx (A_{i,\parallel} - A_{i,\perp})/3A_{i,0}$, where $i = 1$ or 2 denotes the absorbing component, along with the relation $A_{i,\parallel} - A_{i,\perp} = 2(A_{i,0} - A_{i,\perp})$. The latter expression is useful for separating A_1 and A_2 .

Aqueous dispersion of CoMoCat SWCNTs (Southwest Nanotechnologies Inc.,⁸ batch NI-6-A001) was achieved by sonication in buffered salt solution in the presence of 30-mer 5'-GT(GT)₁₃GT-3' single-stranded DNA (Integrated DNA Technologies) followed by centrifugation.^{9,10} Length fractions were generated by size-exclusion chromatography^{11,12}

^{a)} Author to whom correspondence should be addressed. Tel.: (301) 975-6740. FAX: (301) 975-4924. Electronic mail: jeffrey.fagan@nist.gov

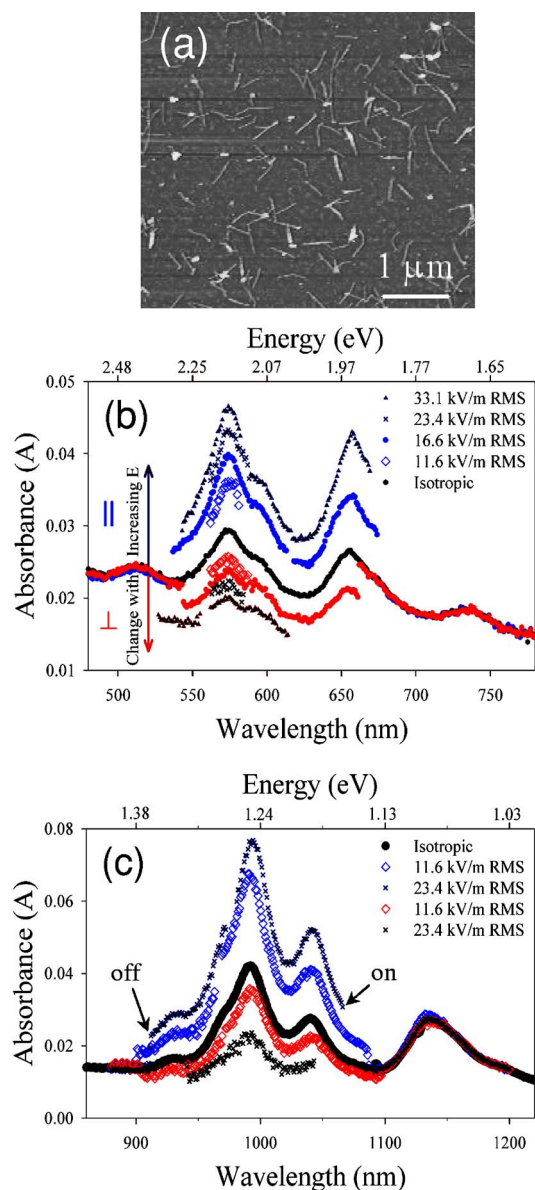


FIG. 1. (Color online) (a) AFM image of the sorted ssDNA-wrapped SWCNTs on mica. (b) Dichroic spectra at the second interband (22) transitions of the $\langle L \rangle = 370$ nm SWCNTs in electric fields of varying strength at a frequency of 3 kHz. Solid black markers are for an isotropic ($E=0$) suspension. Markers above this curve denote polarization parallel (\parallel) to the direction of the applied field, and markers below this curve denote polarization perpendicular (\perp) to the direction of the applied field. (c) A similar plot at the first (11) interband transitions. Discontinuities mark the application (“on”) and subsequent removal (“off”) of E . Note that the absolute intensity of the (6,5) 11 absorption peak is larger than that of the 22 transition.

One single fraction containing longer SWCNTs was chosen for this work. The suspensions were further processed by dialysis through a 50 k-Dalton membrane against 18 M Ω /cm distilled water, which reduced the overall conductivity to <100 μ S/cm and removed the free DNA. Solutions were subsequently diluted with 18 M Ω water until the conductivity was <8 μ S/cm. Total tube concentration was kept small (~ 1 μ g/ml) to reduce tube-tube interactions.

Atomic force microscopy (AFM) and multiple-angle light scattering¹² (MALS) were used to characterize the size distribution. Figure 1(a) shows a typical AFM image of the single stranded DNA (ssDNA) coated SWCNTs on mica. The preponderance of SWCNTs are individuals. The average length¹³ of the fractionated SWCNTs was $\langle L \rangle = 368 \pm 62$ nm

(AFM) and $\langle L \rangle = 329 \pm 35$ nm (MALS) with an effective diameter $d \approx 1$ nm. The Gaussian length distribution has a polydispersity index of 1.2. Ultraviolet/visible/near-infrared (UV-vis-NIR) absorption spectroscopy was performed in transmission mode on a Perkin Elmer Lambda 950 over the range of 1880–190 nm. The instrument was corrected for dark current and background spectra and the reference beam was left unobstructed during the measurement, with the subtraction of the appropriate reference sample performed during data reduction. Spectra were recorded in 1 nm increments with an integration time of 0.04 s per increment. Polarized incident light was selected using a Glan-Thompson polarizer with electronic rotation mount ($\pm 0.2^\circ$). Measurements were made alternating the 270° (parallel to E) and 180° (perpendicular to E) orientations of the polarizer. For $E=0$, measurements at 270° , 225° , 180° , and without the polarizer yield identical spectra.

The electro-optical cell consists of two quartz plates separated by a U shaped poly(dimethyl-siloxane) spacer into which two parallel silver wires are inserted. The horizontal spacing of the two electrodes was 16.2 mm; the width of the light path was 2 mm, centered equidistant between the electrodes. The field was expected to be nearly spatially uniform in the measurement window. The total volume of the cell was ~ 2.2 ml, with roughly 1/2 of the volume outside of the wires to reduce the effects of Joule heating and to provide a reservoir of SWCNTs for diffusional exchange with those in the field. The electric field was generated using a function generator with a high-voltage amplifier (Trek 20/20) and monitored using an oscilloscope. During the experiment, an unbiased alternating electric field was applied for 2.5 s, with each run separated by more than 5 min. Under these conditions, no significant Joule heating, aggregation, or bundling was observed, with no hysteresis or additional time dependence in the results.

Application of an electric field results in the orientation of the SWCNTs as measured by the dichroism of the solution [Figs. 1(b) and 1(c)]. The peak absorption increases along the direction of the field and decreases perpendicular to this. That the time scale of the alignment is short relative to the measurement time of 40 ms can be seen from the sharp transition observed upon application—and subsequent removal—of E . In general, only one point on each end displays an intermediate value. Typical measurements of induced SWCNT birefringence show alignment time scales on the order of 10 ms, implying that the response represents a steady-state distribution of orientations. Increasing E increases the dichroism, and therefore the alignment.

The absorption spectra in Fig. 1 show peaks corresponding to excitonic optical transitions in SWCNTs of specific chirality index (n, m) . As noted above, the lowest energy of these is denoted 11 and the second lowest 22. By measuring the dichroism at these distinct transitions, the extent of alignment can be measured for specific chiralities. Because the semiconducting SWCNTs have multiple electronic transitions in the measured spectrum, the dichroism of the *same* SWCNTs can be observed at different wavelengths to sample independent measures of orientation. Two measures of S are available, $S_{\parallel} \approx (A_{\parallel} - A_0)/2A_0$ and $S_{\perp} \approx (A_0 - A_{\perp})/A_0$. If the intrinsic SWCNT optical coefficients are unaltered by E , then these expressions yield identical measures of alignment, with $S = (S_{\parallel} + S_{\perp})/2$. The dichroism of the (6,5) SWCNT at the 22 absorption feature yields an order parameter, as depicted in

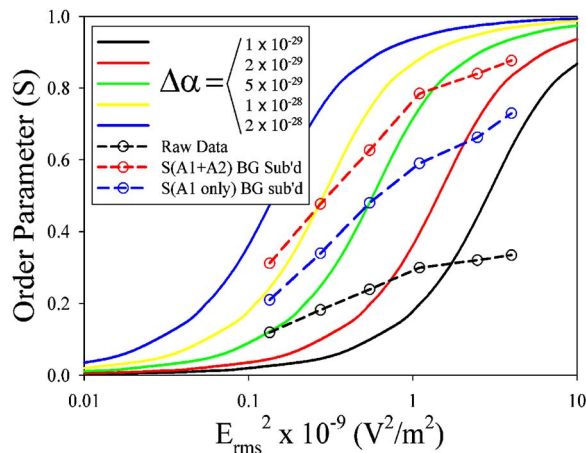


FIG. 2. (Color online) $S(E^2)$ measured at the 22 peak for three types of data analysis. The lower dashed curve is directly calculated from the data in Fig. 1(b) while the upper dashed curve uses background corrected data but does not separate out the alignment of the background. The (correct) middle dashed curve represents the best fit after the removal of the contribution from the broadband absorption, A_2 . The solid curves are the theoretical predictions for different anisotropic polarizabilities (in F m^2), the data suggesting a low- E asymptotic value of $8 \times 10^{-29} \text{ F m}^2$.

Fig. 2. Absorbance measured with the incident light polarized parallel and perpendicular to E give the same degree of alignment for both A_1 and A_2 , and the average of these two values is used. The asymptotic behavior of S at low field strengths is typically used to determine the anisotropic polarizability. For the (6,5) SWCNT (22 peak at 576 nm) this behavior indicates an anisotropy in the polarizability of $\sim(8 \pm 4) \times 10^{-29} \text{ F m}^2$. This value is significantly larger than the literature value for either a dielectric rod ($\sim 6.9 \times 10^{-30} \text{ F m}^2$ for tobacco mosaic virus with $\langle L \rangle \approx 300 \text{ nm}$ and $L/d \approx 20$) or for a conducting rod ($1.2 \times 10^{-29} \text{ F m}^2$ for a gold rod with $\langle L \rangle \approx 300 \text{ nm}$ and $L/d \approx 50$), but is consistent with that calculated for gold rods using the proposed $(L/d)^{0.5}$ to $(L/d)^2$ scaling for conducting and dielectric particles, respectively.^{5,6,14} The value here is larger than the value calculated in Ref. 3, $\Delta\alpha \approx 2.2 \times 10^{-30} \text{ F m}^2$; however, the authors of Ref. 3 state that it is unclear how different SWCNT types are contributing to their measurement. This has the effect of limiting the calculation of $\Delta\alpha$ to only the minimum possible value. The value measured here will be influenced by the interfacial electrostatics of the single-stranded DNA coating in the aqueous environment.

The approach used here gives a measure of S without *a priori* knowledge of the SWCNT volume fraction or optical anisotropy. The only requirement is a large intrinsic optical absorption anisotropy, which has already been demonstrated for the (6,5) SWCNT.⁷ Additionally, the values of S reported here are absolute and represent the response of isolated individual nanotubes. As shown in Fig. 3, approximately equal measures of S are obtained regardless of which transition (11 or 22) is used, suggesting that there is no field-induced change in the intrinsic optical response. Known as the quantum-confined Stark effect, such changes have been reported for SWCNTs in a thin-film transistor configuration with E normal to the SWCNT long axis, albeit at larger fields than those used here.¹⁵ It is anticipated, however, that such

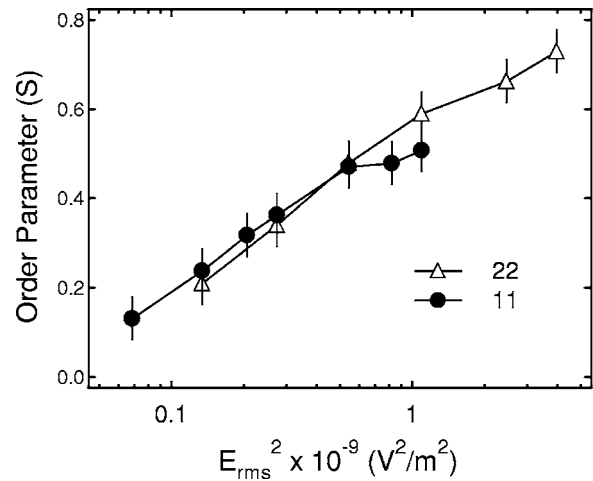


FIG. 3. Comparison of $S(E^2)$ obtained from the response at the first (11) and second (22) interband transitions. Points are from an average of S measured in each polarization configuration.

effects might occur at smaller fields when E is directed along the nanotube.¹⁶ The onset of such an effect might be apparent as a small drop in S deduced from the 11 peak as compared to the 22 peak (Fig. 3), suggestive of a field-induced decrease in the oscillator strength of the more susceptible 11 transition (although there is no apparent shift in the position of the 11 absorption peak). Our results are not sensitive enough to delineate such higher-order effects, however, and we note that they are undesirable here as they would mask the aligning effect of the field.

¹Carbon Nanotubes: Synthesis, Structure, Properties, and Applications, edited by M. S. Dresselhaus, G. Dresselhaus, and P. Avouris (Springer, Heidelberg, 2001).

²K. Bubke, H. Gnewuch, M. Hempstead, J. Hammer, and M. L. H. Green, Appl. Phys. Lett. 71, 1906 (1997).

³K. Donovan and K. Scott, Phys. Rev. B 72, 195432 (2005).

⁴M. S. Brown, J. W. Shan, C. Lin, and F. M. Zimmermann, Appl. Phys. Lett. 90, 203108 (2007).

⁵B. M. I. van der Zande, G. J. M. Koper, and H. N. W. Lekkerkerker, J. Phys. Chem. B 103, 5754 (1999).

⁶C. T. O'Konski, K. Yoshioka, and W. H. Orttung, J. Phys. Chem. 63, 1558 (1959).

⁷J. A. Fagan, J. R. Simpson, B. J. Landi, L. Richter, I. Mandelbaum, J. Obrzut, V. Bajpai, R. Raffaele, B. J. Bauer, A. R. Hight Walker, and E. K. Hobbie, Phys. Rev. Lett. 98, 147402 (2007).

⁸Commercial information is provided only to specify experimental details and does not imply endorsement by NIST or the Department of Commerce.

⁹J. A. Fagan, B. J. Landi, I. Mandelbaum, J. R. Simpson, V. Bajpai, B. J. Bauer, K. Migler, A. R. Hight Walker, R. Raffaele, and E. K. Hobbie, J. Phys. Chem. B 110, 23801 (2006).

¹⁰M. Zheng, A. Jagota, M. S. Strano, A. P. Santos, P. Barone, S. G. Chou, B. A. Diner, M. S. Dresselhaus, R. S. McLean, G. B. Onoa, G. G. Samsonidze, E. D. Semke, M. Usrey, and D. J. Walls, Science 302, 1545 (2003).

¹¹X. Y. Huang, R. S. McLean, and M. Zheng, Anal. Chem. 77, 6225 (2005).

¹²J. A. Fagan, J. R. Simpson, B. J. Bauer, S. Lacerda, M. L. Becker, K. Migler, A. R. Hight Walker, and E. K. Hobbie, J. Am. Chem. Soc. 129, 10607 (2007).

¹³The noted standard uncertainty represents twice the standard deviation calculated, as described or referenced in the manuscript.

¹⁴A. M. Zhivkov, B. M. I. van der Zande, and S. P. Stoylov, Colloids Surf., A 209, 299 (2002).

¹⁵T. Takenobu, Y. Murayama, and Y. Iwasa, Appl. Phys. Lett. 89, 263510 (2006).

¹⁶H. Kishida, H. Matsuzaki, H. Okamoto, T. Manabe, M. Yamashita, Y. Taguchi, and Y. Tokura, Nature (London) 405, 929 (2000).